

ARGONNE NATIONAL LABORATORY
9700 South Cass Avenue
Argonne, Illinois 60439

Convergence Analysis of Fixed Point Chance Constrained Optimal Power Flow Problems

J. J. Brust, M. Anitescu

Mathematics and Computer Science Division

Preprint ANL/MCS-P9431-0121

January 2022

arXiv:2101.11740v3 [math.OC] 17 Jan 2022

¹This work was supported by the U.S. Department of Energy, Office of Science, Advanced Scientific Computing Research, under Contract DE-AC02-06CH11357 at Argonne National Laboratory.

²J. J. Brust is now at Department of Mathematics, University of California, San Diego, CA.

The submitted manuscript has been created by UChicago Argonne, LLC, Operator of Argonne National Laboratory (“Argonne”). Argonne, a U.S. Department of Energy Office of Science laboratory, is operated under Contract No. DE-AC02-06CH11357. The U.S. Government retains for itself, and others acting on its behalf, a paid-up nonexclusive, irrevocable worldwide license in said article to reproduce, prepare derivative works, distribute copies to the public, and perform publicly and display publicly, by or on behalf of the Government. The Department of Energy will provide public access to these results of federally sponsored research in accordance with the DOE Public Access Plan. <http://energy.gov/downloads/doe-public-accessplan>

Convergence Analysis of Fixed Point Chance Constrained Optimal Power Flow Problems

Johannes J. Brust, and Mihai Anitescu, *Member, IEEE*

Abstract—For optimal power flow problems with chance constraints, a particularly effective method is based on a fixed point iteration applied to a sequence of deterministic power flow problems. However, a priori, the convergence of such an approach is not necessarily guaranteed. This article analyses the convergence conditions for this fixed point approach, and reports numerical experiments including for large IEEE networks.

Index Terms—Fixed point method, Chance Constraints, Stochastic Optimizations, AC Optimal Power Flow

I. INTRODUCTION

CHANCE constrained optimization problems are often computationally very challenging. However, when modeling the effects of uncertainty on optimal power networks, potentially large chance constrained optimization problems arise [1]–[5]. Typically, stochastic optimal power flow models are developed by reformulating a widely accepted deterministic model. One such “classical” model is the AC optimal power flow model (AC-OPF) [6]. Because AC-OPF has multiple degrees of freedom with respect to the problem variables, various stochastic power flow paradigms can be derived from it. In particular, one can define different subsets of variables as stochastic variables. For instance, in [7] power generation is regarded as being stochastic (with constant demands), resulting in probabilistic objective functions. This article develops a chance constrained AC optimal power flow model (CC-AC-OPF) in which the objective function is deterministic, and the demands can be stochastic. This enables direct interpretation of the meaning of the optimal objective function values, and can be more realistic, when in practice demand is more of an uncertainty source as compared to supply. Yet, independent of how the stochastic power flow model is formulated it typically yields a chance constrained optimization problem. In order to also solve large instances of the resulting CC-AC-OPF problems, a fixed point iteration on a sequence of modified, related, and simpler deterministic AC-OPF problems is solved. Iterative methods that solve a sequence of simpler problems have been very effective on a variety of recent power systems problems [8]–[10]. In the context of chance-constrained optimization, such an approach has been successfully used in [11]–[13] among more. However, prior to this work, there did not exist analytical criteria for when one can expect this fixed point iteration to converge. Therefore, this article describes a convergence analysis of the chance

constrained fixed point iteration and tests the method on a set of standard IEEE networks. The numerical experiments report results for networks with up to 9000 nodes. To summarize, the contributions of this work are: (1) The formulation of a new CC-AC-OPF model with a deterministic objective function, derived from uncertain demands; (2) The application and analysis of a fixed-point algorithm for an implicit chance constrained problem. Even though the use of iterative (fixed-point) techniques is widespread in power systems problems, previously no rigorous analysis had been undertaken for this formulation. In particular, we disentangle effects of model parameters and network properties on the convergence; (3) We include numerical experiments on large test cases. The article is organized as follows: Sections I.A–D are preliminary and review the AC optimal power flow model and how a chance-constrained model is obtained from it. Section II lists the fixed-point algorithm. We highlight that the reformulation and iterative solution of chance-constrained AC-OPF has been proposed in [11], however a rigorous analysis of its convergence has not yet been developed. Therefore, Section III analyzes convergence properties of the fixed-point algorithm, while numerical experiments are described in Section IV. Finally, we conclude with Section V.

A. AC Power Flow (Preliminary)

The power network is defined by N nodes (buses) and N_{line} edges (lines). Associated to each bus is a voltage magnitude, v_i , frequency θ_i and power generation or consumption at the i^{th} bus, for $1 \leq i \leq N$. In particular, let p_i^g be the real power generated at bus i , q_i^g the corresponding reactive power and p_i^d , q_i^d the real and reactive demands, respectively. The buses are furthermore divided into two groups: generators and loads. The indexing sets are G , and L , which are related to the set of all buses by $B = G \cup L$ (also $N = N_G + N_L$). Throughout, we will use the indexing sets $\{G, L\}$ as subscripts to bold font vector variables. Note that in our setup each bus fits exactly into one of the two categories (though one can easily set a virtual zero load at a node). It is customary to assume that the network contains one reference bus (typically at $i = 1$). Load buses do not have active power generation and are thus defined by $\mathbf{p}_L^g = \mathbf{q}_L^g = \mathbf{0}$, where $\mathbf{p}^g, \mathbf{q}^g$ are vectors that contain the p_i^g 's and q_i^g 's. The power flow in the system is described by the power flow equations, which couple the variables (e.g., [6, Sections III-IV]). Specifically, let G_{ik}, B_{ik} denote the entries of the network's admittance matrix and define the quantities $\theta^{ik} \equiv \theta_i - \theta_k$, $c_{ik} \equiv G_{ik} \cos(\theta^{ik}) + B_{ik} \sin(\theta^{ik})$ and $d_{ik} \equiv G_{ik} \sin(\theta^{ik}) - B_{ik} \cos(\theta^{ik})$. With these definitions, the $2N$

J.J. Brust and M. Anitescu were with Argonne National Laboratory, Mathematics and Computer Science Division upon completion of this article, Lemont, IL, e-mails: jjbrust@ucsd.edu, anitescu@mcsl.anl.gov

This work was supported by the U.S. Department of Energy, Office of Science, Advanced Scientific Computing Research, under Contract DE-AC02-06CH11357 at Argonne National Laboratory.

power flow equations, for $i = 1, \dots, N$, are

$$\begin{aligned} v_i \sum_{k=1}^N v_k c_{ik} - (p_i^g - p_i^d) &= 0, \\ v_i \sum_{k=1}^N v_k d_{ik} - (q_i^g - q_i^d) &= 0, \end{aligned} \quad (1)$$

when grouped by busses. If we let $\mathbf{d} = \text{vec}(\mathbf{p}^d, \mathbf{q}^d)$ be the \mathbb{R}^{2N} vector containing p_i^d, q_i^d then in vector notation (1) is expressed as $\mathbf{f}(\mathbf{v}, \boldsymbol{\theta}, \mathbf{p}^g, \mathbf{q}^g; \mathbf{d}) = \mathbf{0}$, where \mathbf{f} represents the nonlinear equations in (1). Note, however, that \mathbf{f} is linear in \mathbf{d} , a fact we will use later. Moreover, \mathbf{d} is regarded as a parameter and not a variable.

B. AC Optimal Power Flow (Preliminary)

Optimal power flow determines the best set of variables that satisfy the network constraints. In addition to the power flow equations from (1), branch current bounds are typically included in the optimization problem. In particular, let LC be the set of all line connections, i.e., the set of index pairs that describe all line connections (e.g., if bus i is connected to bus k , then $(i, k) \in LC$). Subsequently, the so-called branch current constraints are $(D_{ik}^{\max})^2 - (v_i \cos(\theta_i) - v_k \cos(\theta_k))^2 - (v_i \sin(\theta_i) - v_k \sin(\theta_k))^2 \geq 0$, $\forall (i, k) \in LC$ for constant current limits D_{ik}^{\max} . In vector notation these N_{line} constraints are represented as $\mathbf{g}(\mathbf{v}, \boldsymbol{\theta}) \geq \mathbf{0}$. It is also desirable to include ‘‘hard’’ bounds on the generation variables, such as $\mathbf{l}_p \leq \mathbf{p}_G^g \leq \mathbf{u}_p$, where $\mathbf{l}_p, \mathbf{u}_p$ represent constant lower and upper bounds. The AC optimal power flow (AC-OPF) problem, for a cost function $C_0(\cdot)$, is thus formulated as

$$\begin{aligned} &\underset{\mathbf{v}, \boldsymbol{\theta}, \mathbf{p}^g, \mathbf{q}^g}{\text{minimize}} \quad C_0(\mathbf{p}_G^g) \quad \text{subject to} & (2) \\ \mathbf{f}(\mathbf{v}, \boldsymbol{\theta}, \mathbf{p}^g, \mathbf{q}^g; \mathbf{d}) &= \mathbf{0} & (3) \\ \mathbf{g}(\mathbf{v}, \boldsymbol{\theta}) &\geq \mathbf{0} \\ \mathbf{l}_p &\leq \mathbf{p}_G^g \leq \mathbf{u}_p \\ \mathbf{l}_q &\leq \mathbf{q}_G^g \leq \mathbf{u}_q \\ \mathbf{l}_v &\leq \mathbf{v} \leq \mathbf{u}_v \\ \mathbf{l}_\theta &\leq \boldsymbol{\theta} \leq \mathbf{u}_\theta \end{aligned}$$

The cost function is typically a convex quadratic function that only depends on the real power generation. Specifically, $C_0(\mathbf{p}_G^g) = \sum_{i \in G} q_{ii} (p_i^g)^2 + \sum_{i \in G} q_i p_i^g + q_{00}$ for cost data q_{ii}, q_i and q_{00} . A local solution $\mathbf{s}^* = \text{vec}(\mathbf{v}^*, \boldsymbol{\theta}^*, (\mathbf{p}^g)^*, (\mathbf{q}^g)^*)$ of (2) is called the optimal power flow point, or OPF point.

C. Chance Constrained AC Optimal Power Flow (Preliminary)

In order to introduce uncertainty related to e.g., renewable energy into the OPF problem (2) we regard the demand terms in (1) (i.e., p_i^d, q_i^d) as forecasted values with possible error. Specifically, these stochastic quantities are represented as

$$p_i^d + \omega_i, \quad q_i^d + \omega_{N+i}, \quad (4)$$

where ω_i and ω_{N+i} represent forecasting errors. For compactness, the stochastic errors are represented by the $2N$ vector

$\boldsymbol{\omega}$. Here we assume $\boldsymbol{\omega}$ is normal, and relaxing this assumption yields different approaches. The chance constrained AC-OPF model in this Section is developed such that the objective function only depends on deterministic variables. When the objective function represents cost, deterministic values are meaningful and important. Since the power flow equations in (1) are overdetermined, i.e., $\mathbf{f} : \mathbb{R}^{2N+N_G} \rightarrow \mathbb{R}^{2N}$, this system has N_G degrees of freedom. Subsequently, let $\mathbf{y} = \mathbf{p}_G$ represent a \mathbb{R}^{N_G} vector of deterministic variables and $\mathbf{x} = \mathbf{x}(\boldsymbol{\omega}) = \text{vec}(\mathbf{q}_G(\boldsymbol{\omega}), \mathbf{v}_L(\boldsymbol{\omega}), \boldsymbol{\theta}(\boldsymbol{\omega}))$ a $2N$ vector of stochastic variables. The stochastic power flow equations are represented as

$$\mathbf{f}(\mathbf{x}, \mathbf{y}; \mathbf{d}) + \boldsymbol{\omega} = \mathbf{f}_\omega(\mathbf{x}(\boldsymbol{\omega}), \mathbf{y}; \mathbf{d} + \boldsymbol{\omega}) \equiv \mathbf{f}_\omega = \mathbf{0}. \quad (5)$$

If $\boldsymbol{\omega} = \mathbf{0}$ these equations reduce to the power flow equations in (1). Note that the power flow equations couple the variables and that the uncertainty in \mathbf{x} depends on the uncertainty in the demands ‘‘ \mathbf{d} ’’, since $\mathbf{x} = \mathbf{x}(\boldsymbol{\omega}) = \mathbf{x}(\mathbf{y}, \mathbf{d} + \boldsymbol{\omega})$. We set $C_0(\mathbf{p}_G^g) = C_0(\mathbf{y})$ to reflect the change in variables for the stochastic optimal power flow problem and note that the objective function is deterministic. Let $\mathbb{P}(\mathbf{z} \geq \mathbf{0}) \geq 1 - \epsilon$ represent a vector of inequalities with non-negative probability constraints, for which each element in the left hand side corresponds to a cumulative probability (for $z_i \geq 0$) and each element of ϵ is in the interval $0 < \epsilon < 1$. Then the chance constrained (stochastic) optimal power flow problem is given by

$$\begin{aligned} &\underset{\mathbf{x}(\boldsymbol{\omega}), \mathbf{y}}{\text{minimize}} \quad C_0(\mathbf{y}) \quad \text{subject to} & (6) \\ \mathbf{f}_\omega(\mathbf{x}(\boldsymbol{\omega}), \mathbf{y}; \mathbf{d} + \boldsymbol{\omega}) &= \mathbf{0} & \forall \boldsymbol{\omega} \\ \mathbb{P}(\mathbf{g}(\mathbf{x}(\boldsymbol{\omega}), \mathbf{y}) \geq \mathbf{0}) &\geq 1 - \epsilon_g & (7) \\ \mathbb{P}(\mathbf{l}_x \leq \mathbf{x}(\boldsymbol{\omega}) \leq \mathbf{u}_x) &\geq 1 - \epsilon_x & (8) \\ \mathbf{l}_y &\leq \mathbf{y} \leq \mathbf{u}_y. \end{aligned}$$

Observe that the problem in (6) includes chance constraints (probability constraints) on the line flow limits (7) and the stochastic variables $\mathbf{x}(\boldsymbol{\omega})$ (8), while deterministic limits are set on \mathbf{y} . Here ϵ_g and ϵ_x correspond to model parameters for setting probability thresholds.

1) *Computing Chance Constraints:* To practically compute the chance constraints in problem (6), the stochastic variables are linearized around the error $\boldsymbol{\omega}$ (zero mean). This is equivalent to assuming that $\boldsymbol{\omega}$ is sufficiently small, which we proceed to do in the rest of the paper. In particular,

$$\mathbf{x}(\mathbf{y}, \mathbf{d} + \boldsymbol{\omega}) \approx \mathbf{x}(\mathbf{y}, \mathbf{d}) + \left. \frac{\partial \mathbf{x}(\mathbf{y}, \mathbf{d} + \boldsymbol{\omega})}{\partial \boldsymbol{\omega}} \right|_{\boldsymbol{\omega}=\mathbf{0}} \boldsymbol{\omega} \equiv \mathbf{x}_\omega. \quad (9)$$

Note that $\mathbf{x}(\mathbf{y}, \mathbf{d}) = \mathbf{x}_0$ and that $\partial \mathbf{x}(\mathbf{y}, \mathbf{d}) / \partial \boldsymbol{\omega}$ are deterministic. Thus the expectation and variance of \mathbf{x}_ω are $\mathbb{E}[\mathbf{x}_\omega] = \mathbf{x}(\mathbf{y}, \mathbf{d}) = \mathbf{x}_0$, and $\text{Var}[\mathbf{x}_\omega] = (\partial \mathbf{x}(\mathbf{y}, \mathbf{d}) / \partial \boldsymbol{\omega}) \text{Var}[\boldsymbol{\omega}] (\partial \mathbf{x}(\mathbf{y}, \mathbf{d}) / \partial \boldsymbol{\omega})^\top$, respectively. Alternatively, more accurate dynamics of the stochastic variables may be based on a 2nd order expansion $\mathbf{x}(\mathbf{y}, \mathbf{d} + \boldsymbol{\omega}) \approx \mathbf{x}(\mathbf{y}, \mathbf{d}) + (\partial \mathbf{x} / \partial \boldsymbol{\omega}) \boldsymbol{\omega} + \text{‘‘second order terms’’}$. When the covariance of the uncertainty has a particular structure (e.g., diagonal) then the mean of the expansion can be determined analytically. The expansion’s covariance is more involved and may need to be

estimated. Another possibility to include nonlinearities might be a quadratic model of the load: $\omega_3 \cdot * (\mathbf{p}^d)^{\cdot 2} + \omega_2 \cdot * (\mathbf{p}^d) + \omega_1$, where $\cdot *$ and \cdot^2 are element-wise multiplications and squares. For computational efficiency we use the probabilities of the linearized random variables. For instance, the constraints from (8) are written as

$$\mathbb{P}(\mathbf{x}_\omega \leq \mathbf{u}_x) \geq \mathbf{1} - \boldsymbol{\epsilon}_x, \quad \mathbb{P}(\mathbf{l}_x \leq \mathbf{x}_\omega) \geq \mathbf{1} - \boldsymbol{\epsilon}_x. \quad (10)$$

To handle the vector of probabilities in (10) one can use a Bonferroni bound [14], in which each individual variable $(\mathbf{x}_\omega)_r$ for $1 \leq r \leq 2N$ satisfies an individual highly conservative probability constraint. However, when the variables are independent (or can be treated as such) then the probabilities can be separated without restrictions. The mean of $(\mathbf{x}_\omega)_r$ is $(\mathbf{x}_0)_r$, while the variance can also be explicitly computed. Define

$$\partial \mathbf{x} / \partial \boldsymbol{\omega} \equiv \boldsymbol{\Gamma}, \quad (11)$$

and let \mathbf{e}_r be the r^{th} column of the identity matrix. Moreover, denote $\text{Var}[\boldsymbol{\omega}] = \boldsymbol{\Sigma}^2$. With this the variance of $(\mathbf{x}_\omega)_r$ is $\|\mathbf{e}_r^\top \boldsymbol{\Gamma} \boldsymbol{\Sigma}\|_2^2$. In turn, when the variables can be treated independently, individual probability constraints, such as $F^{\text{Nrm}}((\mathbf{x}_\omega)_r \leq (\mathbf{u}_x)_r) \geq 1 - (\boldsymbol{\epsilon}_x)_r$ (where F^{Nrm} is the normal distribution function) can be represented as

$$((\mathbf{u}_x)_r - (\mathbf{x}_0)_r) / \|\mathbf{e}_r^\top \boldsymbol{\Gamma} \boldsymbol{\Sigma}\|_2 \geq (F^{\text{Nrm}})^{-1}(1 - (\boldsymbol{\epsilon}_x)_r),$$

where $(F^{\text{Nrm}})^{-1}(\cdot)$ is the inverse cumulative distribution function. Defining $z_r = (F^{\text{Nrm}})^{-1}(1 - (\boldsymbol{\epsilon}_x)_r)$ the constraints are represented as

$$(\mathbf{u}_x)_r - \lambda_r \geq (\mathbf{x}_0)_r, \quad \lambda_r = z_r \|\mathbf{e}_r^\top \boldsymbol{\Gamma} \boldsymbol{\Sigma}\|_2. \quad (12)$$

Similarly, for $2N + 1 \leq r_1 \leq 2N + N_L$ and $\bar{r}_1 = r_1 - 2N$, defining $z_{r_1} = (F^{\text{Nrm}})^{-1}(1 - (\boldsymbol{\epsilon}_g)_{r_1})$ the remaining probability constraints are represented as $\mathbf{g}(\mathbf{x}_0, \mathbf{y})_{\bar{r}_1} - \lambda_{r_1} \geq \mathbf{0}$ with

$$\lambda_{r_1} = z_{r_1} \|\mathbf{e}_{\bar{r}_1}^\top (\partial \mathbf{g} / \partial \mathbf{x}) \boldsymbol{\Gamma} \boldsymbol{\Sigma}\|_2. \quad (13)$$

Note that λ_r, λ_{r_1} depend on \mathbf{x}, \mathbf{y} and \mathbf{d} , e.g., $\lambda_r = \lambda_r(\mathbf{x}(\mathbf{y}, \mathbf{d}))$, which we will use later. Moreover the inequality in (12) is deterministic and thus straightforward to compute once $\boldsymbol{\Gamma}$ is known. Second, when $(\boldsymbol{\epsilon}_x)_r$ is a small number (which is typically the case) then $z_r > 0$ and $\lambda_r > 0$. Thus the λ_r, λ_{r_1} values are regarded as constraint tightenings and represent the effects of stochasticity in the constraints. Note that when other distributions are desired, one can substitute the $(F^{\text{Nrm}})^{-1}(\cdot)$ c.d.f. (above (12) and elsewhere) with another one. Since investigations about distributional robustness have been previously conducted by other researchers we refer to [15, Sec. III.A] for in-depth discussions.

2) *Computing $\partial \mathbf{x} / \partial \boldsymbol{\omega}$* : The partial derivatives $\partial \mathbf{x} / \partial \boldsymbol{\omega} = \boldsymbol{\Gamma}$ in (12) are obtained by using the power flow equation

$$\frac{\partial}{\partial \boldsymbol{\omega}} (\mathbf{f}_\omega(\mathbf{x}(\boldsymbol{\omega}), \mathbf{y}; \mathbf{d} + \boldsymbol{\omega})) = \frac{\partial \mathbf{f}_\omega}{\partial \mathbf{x}} \frac{\partial \mathbf{x}}{\partial \boldsymbol{\omega}} + \frac{\partial \mathbf{f}_\omega}{\partial \boldsymbol{\omega}} = \mathbf{0}.$$

First, note from (5) that $\partial \mathbf{f}_\omega / \partial \boldsymbol{\omega} = \mathbf{I}$. Second, the partial derivatives are only needed at $\boldsymbol{\omega} = \mathbf{0}$, which yields the representation $\partial \mathbf{x} / \partial \boldsymbol{\omega} = -(\partial \mathbf{f}_0 / \partial \mathbf{x})^{-1}$ with the convention

$\mathbf{f}_0 = \mathbf{f}$. Since $\mathbf{x} = \text{vec}(\mathbf{q}_G^g, \mathbf{v}_L, \boldsymbol{\theta})$ the so-called Jacobian matrix of partial derivatives is given by

$$\frac{\partial \mathbf{f}}{\partial \mathbf{x}} = \begin{bmatrix} \frac{\partial \mathbf{f}}{\partial \mathbf{q}_G^g} & \frac{\partial \mathbf{f}}{\partial \mathbf{v}_L} & \frac{\partial \mathbf{f}}{\partial \boldsymbol{\theta}} \end{bmatrix}. \quad (14)$$

The elements of this matrix can be computed from (1). Note that only the last N equations in (1) depend on \mathbf{q}^g . Subsequently, we define the indices $1 \leq i \leq N$ and $j = N + i$, as well as $1 \leq g \leq N_G$, $1 \leq l \leq N_L$ and $1 \leq t \leq N$. With this, the elements of the Jacobian from (14) are:

$$\begin{aligned} \left(\frac{\partial \mathbf{f}}{\partial \mathbf{q}_G^g} \right)_{i,g} &= 0, \\ \left(\frac{\partial \mathbf{f}}{\partial \mathbf{q}_G^g} \right)_{j,g} &= \begin{cases} -1 & \text{if } i = [G]_g \\ 0 & \text{otherwise} \end{cases} \\ \left(\frac{\partial \mathbf{f}}{\partial \mathbf{v}_L} \right)_{i,l} &= \begin{cases} \sum_{k=1}^N v_k c_{ik} + 2c_{ii} v_i & \text{if } i = [L]_l \\ v_i c_{i[L]_l} & \text{otherwise} \end{cases} \\ \left(\frac{\partial \mathbf{f}}{\partial \mathbf{v}_L} \right)_{j,l} &= \begin{cases} \sum_{k=1}^N v_k d_{ik} + 2d_{ii} v_i & \text{if } i = [L]_l \\ v_i d_{i[L]_l} & \text{otherwise} \end{cases} \\ \left(\frac{\partial \mathbf{f}}{\partial \boldsymbol{\theta}} \right)_{i,t} &= \begin{cases} -v_i \sum_{k=1}^N v_k d_{ik} & \text{if } i = t \\ v_i v_t d_{it} & \text{otherwise} \end{cases} \\ \left(\frac{\partial \mathbf{f}}{\partial \boldsymbol{\theta}} \right)_{j,t} &= \begin{cases} v_i \sum_{k=1}^N v_k c_{ik} & \text{if } i = t \\ -v_i v_t c_{it} & \text{otherwise} \end{cases} \end{aligned} \quad (15)$$

The partial derivatives $\partial \mathbf{x} / \partial \boldsymbol{\omega} = (\partial \mathbf{f} / \partial \mathbf{x})^{-1}$ are defined by an inverse. This inverse is typically well defined for regular optimal power flow problems, as described in [7, Section III. B] and [16] (if numerically the Jacobian matrix becomes (nearly) singular, it may be corrected by shifting its diagonal elements by adding a multiple of the identity matrix). Therefore, the smallest singular value of $\partial \mathbf{f} / \partial \mathbf{x} \equiv \mathbf{J}$ is positive, i.e., $\sigma_{\min}(\mathbf{J}) > 0$. A positive lower bound for the smallest singular value of a matrix is described in [17, Theorem 1]. Let $\mathbf{J}_{:,i}$ denote the i^{th} column of \mathbf{J} and let $\mathbf{J}_{i,:}$ be the i^{th} row of \mathbf{J} . Then a lower bound for the smallest singular value is:

$$\sigma_{\min}(\mathbf{J}) \geq \hat{K}_\Gamma > 0,$$

where $\hat{K}_\Gamma = \left(\frac{\hat{n}-1}{\hat{n}} \right)^{\frac{\hat{n}-1}{2}} |\mathbf{J}| \max \left(\frac{\min(\|\mathbf{J}_{:,i}\|_2)}{\prod_i \|\mathbf{J}_{:,i}\|_2}, \frac{\min(\|\mathbf{J}_{i,:}\|_2)}{\prod_i \|\mathbf{J}_{i,:}\|_2} \right)$, $\hat{n} \equiv 2N$, and where the determinant is $|\mathbf{J}| = \det(\mathbf{J})$. This means that

$$\|(\partial \mathbf{f} / \partial \mathbf{x})^{-1}\|_2 = \|\mathbf{J}^{-1}\|_2 = \frac{1}{\sigma_{\min}(\mathbf{J})} \leq 1 / \hat{K}_\Gamma \equiv K_\Gamma \quad (16)$$

where \hat{K}_Γ, K_Γ are finite constants. In order to compute solves with \mathbf{J} (which is part of computing the constraints in (12) and (13)) the LU factorization is based on the decomposition $\mathbf{J} = \mathbf{P}\mathbf{L}\mathbf{U}$, where \mathbf{P} is a permutation matrix, \mathbf{L} is a unit lower triangular matrix and \mathbf{U} is an upper triangular matrix. The determinant and the bounds in (16) are thus available “without extra expense” based on solves with \mathbf{J} , by multiplying the diagonal elements of \mathbf{U} , since $|\mathbf{J}| = |\mathbf{U}|$ and \mathbf{U} is upper triangular. Since the determinant can often become large (even if a matrix is well conditioned) a possibly preferable approach of computing constant K_Γ is to exploit the inequality $\|\mathbf{J}^{-1}\| \leq \sqrt{\|\mathbf{J}^{-1}\|_1 \|\mathbf{J}^{-1}\|_\infty} \equiv K_\Gamma$. Note that computing K_Γ can be inexpensive since \mathbf{J}^{-1} is computed as part of e.g., (12).

D. Implicit Chance Constrained Optimal Power Flow

An optimal power flow problem that combines components of the AC-OPF problem in (2) and of the chance constrained problem in (6) is obtained by using the constraints from (12) and (13). This reformulated problem incorporates stochastic effects, while at the same time enables efficient computations. The corresponding *implicit* chance-constrained AC-OPF problem is:

$$\begin{aligned} & \underset{\mathbf{v}, \boldsymbol{\theta}, \mathbf{p}^g, \mathbf{q}^g}{\text{minimize}} \quad C_0(\mathbf{p}_G^g) \quad \text{subject to} & (17) \\ & \mathbf{f}(\mathbf{v}, \boldsymbol{\theta}, \mathbf{p}^g, \mathbf{q}^g; \mathbf{d}) = \mathbf{0} \\ & \mathbf{g}(\mathbf{v}, \boldsymbol{\theta}) \geq \boldsymbol{\lambda}_g(\mathbf{p}_G^g) \\ & \mathbf{l}_q + \boldsymbol{\lambda}_q(\mathbf{p}_G^g) \leq \mathbf{q}_G^g \leq \mathbf{u}_q - \boldsymbol{\lambda}_q(\mathbf{p}_G^g) \\ & \mathbf{l}_v + \boldsymbol{\lambda}_v(\mathbf{p}_G^g) \leq \mathbf{v}_L \leq \mathbf{u}_v - \boldsymbol{\lambda}_v(\mathbf{p}_G^g) \\ & \mathbf{l}_\theta + \boldsymbol{\lambda}_\theta(\mathbf{p}_G^g) \leq \boldsymbol{\theta} \leq \mathbf{u}_\theta - \boldsymbol{\lambda}_\theta(\mathbf{p}_G^g) \\ & \mathbf{l}_p \leq \mathbf{p}_G^g \leq \mathbf{u}_p, \end{aligned}$$

where $\boldsymbol{\lambda}_q(\mathbf{p}_G^g)$, $\boldsymbol{\lambda}_v(\mathbf{p}_G^g)$, $\boldsymbol{\lambda}_\theta(\mathbf{p}_G^g)$ are computed using (12) and $\boldsymbol{\lambda}_g(\mathbf{p}_G^g)$ is computed using (13). The problem can be seen to be implicit with regards to probability constraints, because the effects of uncertainty are implicitly included in the tightenings of some constraints by the non-negative $\boldsymbol{\lambda}$'s.

II. METHOD

The solution of the potentially large nonlinear optimization problem in (17) can be computed directly. However, the computation of the $\boldsymbol{\lambda}$'s adds nonlinearities, because they depend on the matrix $\boldsymbol{\Gamma} = -(\partial \mathbf{x} / \partial \boldsymbol{\omega})^{-1} \in \mathbb{R}^{2N \times 2N}$, which is an inverse. Because of this, the problem in (17) is still computationally difficult. Instead of solving (17) directly, an iterative scheme, which computes an approximate solution of (17), by solving a sequence of simpler problems has been proposed in [11]. Such an algorithm is stated as:

Algorithm 1

- 1: Inputs: $\mathbf{s}^{(0)} = \text{vec}(\mathbf{v}^{(0)}, \boldsymbol{\theta}^{(0)}, \mathbf{p}^{(0)}, \mathbf{q}^{(0)})$, $0 < \tau_q$, $0 < \tau_v$, $0 < \tau_\theta$, $0 < \tau_g$, $0 < \epsilon_q \leq 0.5$, $0 < \epsilon_v \leq 0.5$, $0 < \epsilon_\theta \leq 0.5$, $0 < \epsilon_g \leq 0.5$, $0 < \boldsymbol{\Sigma}$, $\boldsymbol{\lambda}_q^{(0)} = \boldsymbol{\lambda}_v^{(0)} = \boldsymbol{\lambda}_\theta^{(0)} = \boldsymbol{\lambda}_g^{(0)} = \mathbf{0}$, $k = 0$;
- 2: for $k = 0, 1, \dots$
- 3: Solve (17) with $\boldsymbol{\lambda}_q^{(k)}, \boldsymbol{\lambda}_v^{(k)}, \boldsymbol{\lambda}_\theta^{(k)}$ fixed and obtain $\mathbf{s}^{(k+1)}$;
- 4: Compute $\boldsymbol{\lambda}_q^{(k+1)}, \boldsymbol{\lambda}_v^{(k+1)}, \boldsymbol{\lambda}_\theta^{(k+1)}, \boldsymbol{\lambda}_g^{(k+1)}$ using (12) and (13);
- 5: **if**

$$\begin{aligned} & \|\boldsymbol{\lambda}_q^{(k+1)} - \boldsymbol{\lambda}_q^{(k)}\|_\infty \leq \tau_q \text{ and} \\ & \|\boldsymbol{\lambda}_v^{(k+1)} - \boldsymbol{\lambda}_v^{(k)}\|_\infty \leq \tau_v \text{ and} \\ & \|\boldsymbol{\lambda}_\theta^{(k+1)} - \boldsymbol{\lambda}_\theta^{(k)}\|_\infty \leq \tau_\theta \text{ and} \\ & \|\boldsymbol{\lambda}_g^{(k+1)} - \boldsymbol{\lambda}_g^{(k)}\|_\infty \leq \tau_g \end{aligned}$$
then
 - 6: Stop. Return $\mathbf{s}^{(k+1)}$;
 - 7: **else**
 - 8: $k = k + 1$;
 - 9: **end if**

Note that Algorithm 1 stops when the changes in the $\boldsymbol{\lambda}$'s become small. However no criteria have yet been specified for when one can expect the iteration to converge. Therefore, we analyze conditions for which one can expect Algorithm 1 to converge.

III. ANALYSIS

The analysis of Algorithm 1 is based on the insight that this iterative algorithm is a fixed point iteration. Therefore, in order to derive its convergence conditions, we investigate the convergence conditions of the fixed point iteration. Throughout this section, the problem from (17) is reformulated as

$$\begin{aligned} & \underset{\mathbf{s}}{\text{minimize}} \quad C_1(\mathbf{s}) \quad \text{subject to} & (18) \\ & \mathbf{f}(\mathbf{s}) = \mathbf{0}, \quad \mathbf{h}(\mathbf{s}; \boldsymbol{\lambda}) \geq \mathbf{0} \end{aligned}$$

with $\mathbf{s} = \text{vec}(\mathbf{v}, \boldsymbol{\theta}, \mathbf{p}^g, \mathbf{q}^g)$, $C_1(\mathbf{s}) = C_0(\mathbf{p}_G^g)$, $\boldsymbol{\lambda} = \boldsymbol{\lambda}(\mathbf{s}) = \text{vec}(\boldsymbol{\lambda}_q, \boldsymbol{\lambda}_v, \boldsymbol{\lambda}_\theta, \boldsymbol{\lambda}_g)$, $\mathbf{h}(\mathbf{s}; \boldsymbol{\lambda}) \geq \mathbf{0} \in \mathbb{R}^m$ ($m = N_L + 4N$ inequality constraints in (17)) and $\mathbf{f}(\mathbf{s}; \mathbf{d}) = \mathbf{f}(\mathbf{s})$. Our analysis is consistent with classical nonlinear programming sensitivity results [18], [19], however is different because of the fixed point component of the algorithm. In classical nonlinear programming $\boldsymbol{\lambda}$ is taken as an independent perturbation parameter, with focus on the sensitivities of \mathbf{s} with respect to $\boldsymbol{\lambda}$. However, because the (implicit) chance-constrained problem also contains the dependence $\boldsymbol{\lambda} = \boldsymbol{\lambda}(\mathbf{s})$ we are led to also acknowledge the interplay of $\boldsymbol{\lambda}$ and \mathbf{s} . Recall that a fixed point, say $\boldsymbol{\lambda}^*$, of a continuous function/mapping, say $M(\boldsymbol{\lambda})$, can be defined by the two conditions

$$\begin{aligned} M(\boldsymbol{\lambda}^*) &= \boldsymbol{\lambda}^*, & \|\partial M(\boldsymbol{\lambda}^*) / \partial \boldsymbol{\lambda}\|_2 &\in [0, 1] & (19) \\ \text{Condition 1} & & \text{Condition 2} & & \end{aligned}$$

(see for instance [20, Sec. 10.1] and [21, Sec. 6.3] on fixed points.) These two conditions are generalizations of a scalar fixed-point (FP) to vector valued functions. Condition 1 represents the definition of a FP, which is a point that remains unchanged after being mapped. Condition 2 is a sufficient condition for a fixed point mapping to converge [20, Theorem 10.6]). This condition implies that recursive mappings of a fixed-point are characterized by vanishing derivatives (successively applying the mapping results in a stable point, which make such mapping be sometimes called a contraction [20, Theorem 10.6]). Note that Algorithm 1 in line 5 checks whether the differences in successive constraint tightenings are small, i.e., this is a numerical check of Condition 1. We further analyze properties of Condition 2 to obtain insights into the convergence behavior of the algorithm. Now, to closer investigate the relation between the variables in Algorithm 1, define the mapping in line 3 that determines $\mathbf{s}^{(k+1)}$ from $\boldsymbol{\lambda}^{(k)}$ by $\mathbf{s}_M(\boldsymbol{\lambda}^{(k)})$ (i.e., $\mathbf{s}^{(k+1)} = \mathbf{s}_M(\boldsymbol{\lambda}^{(k)})$), and the operation in line 4 that determines $\boldsymbol{\lambda}^{(k+1)}$ from $\mathbf{s}^{(k+1)}$ by $\boldsymbol{\lambda}_M(\mathbf{s}^{(k+1)})$ (i.e., $\boldsymbol{\lambda}^{(k+1)} = \boldsymbol{\lambda}_M(\mathbf{s}^{(k+1)})$). Then the statements in the algorithm recursively define the next iterates, starting from $k = 0$, $\mathbf{s}^{(k)}$, $\boldsymbol{\lambda}^{(k)}$, so that,

$$\begin{aligned} \mathbf{s}^{(k+1)} &= \mathbf{s}_M(\boldsymbol{\lambda}^{(k)}), & \boldsymbol{\lambda}^{(k+1)} &= \boldsymbol{\lambda}_M(\mathbf{s}^{(k+1)}) \\ &= \mathbf{s}_M(\boldsymbol{\lambda}_M(\mathbf{s}^{(k)})), & &= \boldsymbol{\lambda}_M(\mathbf{s}_M(\boldsymbol{\lambda}^{(k)})). \end{aligned}$$

This means that there is a mapping that generates $\mathbf{s}^{(k+1)}$ from $\mathbf{s}^{(k)}$ and one that generates $\boldsymbol{\lambda}^{(k+1)}$ from $\boldsymbol{\lambda}^{(k)}$. In particular, if $\boldsymbol{\lambda}^{(k)} \rightarrow \boldsymbol{\lambda}^*$ then $\mathbf{s}^{(k)} \rightarrow \mathbf{s}^*$ and vice-versa. Our analysis is based on the assertion that if Condition 2 in (19) holds, then $\boldsymbol{\lambda}^*$ (and \mathbf{s}^*) is a fixed point.

First, we describe the basic properties of a solution to (18), which enables the use of results from nonlinear programming later on, and also the establishing of reasonable assumptions.

A. Basic Conditions

A solution to the nonlinear programming problem (18) is characterized by a set of conditions for the Lagrangian:

$$L(\mathbf{s}, \boldsymbol{\mu}, \boldsymbol{\rho}; \boldsymbol{\lambda}) = C_1(\mathbf{s}) + \boldsymbol{\mu}^\top \mathbf{f}(\mathbf{s}) + \boldsymbol{\rho}^\top \mathbf{h}(\mathbf{s}; \boldsymbol{\lambda}),$$

where $\boldsymbol{\mu} \in \mathbb{R}^{2N}$ and $\boldsymbol{\rho} \geq \mathbf{0} \in \mathbb{R}^m$. Subsequently, the Karush-Kuhn-Tucker (KKT) [22], [23] optimality conditions are the set of nonlinear conditions that define a solution of (18):

$$\begin{aligned} \frac{\partial}{\partial \mathbf{s}} L(\mathbf{s}, \boldsymbol{\mu}, \boldsymbol{\rho}; \boldsymbol{\lambda}) &= \mathbf{0} \\ \mathbf{f}(\mathbf{s}) &= \mathbf{0} \\ \mathbf{h}(\mathbf{s}, \boldsymbol{\lambda}) &\geq \mathbf{0} \\ \boldsymbol{\rho}_i \mathbf{h}(\mathbf{s}, \boldsymbol{\lambda})_i &= 0, \quad i = 1, \dots, m \\ \boldsymbol{\rho} &\geq \mathbf{0}. \end{aligned} \quad (20)$$

The set of active inequality constraints is defined as

$$\mathcal{A}(\mathbf{s}) = \{i : \mathbf{h}(\mathbf{s}, \boldsymbol{\lambda})_i = 0\}.$$

A solution to (20) can be found when the columns of the constraint Jacobians are linearly independent, i.e., when

$$\left[\begin{array}{cc} \frac{\partial}{\partial \mathbf{s}} \mathbf{f}(\mathbf{s}), & \frac{\partial}{\partial \mathbf{s}} \mathbf{h}(\mathbf{s}, \boldsymbol{\lambda})_i \end{array} \right], \quad i \in \mathcal{A}(\mathbf{s}), \quad (21)$$

are linearly independent. Moreover, second order conditions (which state that the Lagrangian Hessian is positive definite in the nullspace of the constraint derivatives) ensure strict local optimality of a KKT point. Finally, if the active set is unchanged in a small neighborhood around $\boldsymbol{\lambda}$, then changes in \mathbf{s} with regards to changes in $\boldsymbol{\lambda}$ are continuous. Summarizing we assume the three conditions. Assumptions (Analysis):

- A.1: Linear independence in the constraint Jacobians (21)
- A.2: Second order sufficient conditions hold for (18)
- A.3: Strict complementary slackness: $\boldsymbol{\rho}_i > 0, i \in \mathcal{A}(\mathbf{s})$.

The first two assumptions state that a local minimum for the problem in (18) exists. The third ensures continuity of derivatives, such as $\frac{\partial \mathbf{s}}{\partial \boldsymbol{\lambda}}$ and $\frac{\partial \boldsymbol{\lambda}_M}{\partial \boldsymbol{\lambda}}$. We further assume access to a solver that can find a local minimum when it exists. Because of the continuity of partial derivatives the active set at a (local) solution does not change. A numerical investigation of a zig-zag behavior of Algorithm 1 due to a disconnected feasible set can be found in [15]. Note that when changes in the constraint tightenings are not abrupt, but smooth, assuming continuity is reasonable. We like to note that [15, Sec. V.A] empirically observed that in cases where tightenings are small (relative to other terms) the algorithm converged more frequently on linear programs.

B. Analysis Outline

A goal of the analysis is to deduce properties of the quantity $\left\| \frac{\partial \boldsymbol{\lambda}_M}{\partial \boldsymbol{\lambda}} \right\|$ (in order to investigate when Condition 2 in (19) will hold). To achieve this first a representation of $\frac{\partial \boldsymbol{\lambda}_M}{\partial \boldsymbol{\lambda}}$ is needed, which is derived in Part I. Subsequently, the representation of $\frac{\partial \boldsymbol{\lambda}_M}{\partial \boldsymbol{\lambda}}$ depends on changes in variables and constraints that are developed as the sensitivities $\frac{\partial \mathbf{s}}{\partial \lambda_n}$ and $\frac{\partial^2 \mathbf{f}}{\partial \lambda_n \partial \mathbf{x}}$ in Part II. Ultimately, Part III uses the previous outcomes to deduce $\left\| \frac{\partial \boldsymbol{\lambda}_M}{\partial \boldsymbol{\lambda}} \right\|_2$ and implications. (We use the notation $(\boldsymbol{\lambda})_n = \lambda_n$ to denote the n^{th} element of $\boldsymbol{\lambda}$)

Part I: Representation of $\frac{\partial \boldsymbol{\lambda}_M}{\partial \boldsymbol{\lambda}}$

Part II: Sensitivities $\frac{\partial \mathbf{s}}{\partial \lambda_n}$ and $\frac{\partial^2 \mathbf{f}}{\partial \lambda_n \partial \mathbf{x}}$

Part III: Bound on $\left\| \frac{\partial \boldsymbol{\lambda}_M}{\partial \boldsymbol{\lambda}} \right\|_2$ and Implications

To develop a representation for $\frac{\partial \boldsymbol{\lambda}_M}{\partial \boldsymbol{\lambda}}$ we analyze the expression

$$(\boldsymbol{\lambda}_M(\mathbf{s}(\boldsymbol{\lambda})))_r = z_r \|\mathbf{e}_r^\top \boldsymbol{\Gamma}(\mathbf{s}(\boldsymbol{\lambda})) \boldsymbol{\Sigma}\|_2,$$

which is (12) with explicit dependencies on \mathbf{s} and $\boldsymbol{\lambda}$. (The conditions for (13) are done in a similar way, with an additional constant for the derivatives of the line flow constraints: $\|\partial \mathbf{g} / \partial \mathbf{x}\|_2 \leq K_g$).

C. Part I: Representation of $\frac{\partial \boldsymbol{\lambda}_M}{\partial \boldsymbol{\lambda}}$

In this section we first make the relation between \mathbf{s} and $\boldsymbol{\lambda}$ explicit. Thus the $\boldsymbol{\Gamma}$ matrix is represented as a function of \mathbf{s} and $\boldsymbol{\lambda}$ i.e., $\boldsymbol{\Gamma}(\mathbf{s}(\boldsymbol{\lambda})) = -\mathbf{J}(\mathbf{s}(\boldsymbol{\lambda}))^{-1}$, where $\mathbf{J}(\mathbf{s}(\boldsymbol{\lambda})) = \mathbf{J} = \partial \mathbf{f} / \partial \mathbf{x}$ (cf. (14)). For notation, we will be using the following definition

$$\mathbf{w}_r(\mathbf{s}(\boldsymbol{\lambda})) \equiv \boldsymbol{\Sigma} \boldsymbol{\Gamma}(\mathbf{s}(\boldsymbol{\lambda}))^\top \mathbf{e}_r, \quad (22)$$

and write $(\boldsymbol{\lambda}_M(\mathbf{s}(\boldsymbol{\lambda})))_r = z_r [\mathbf{w}_r(\mathbf{s}(\boldsymbol{\lambda}))^\top \mathbf{w}_r(\mathbf{s}(\boldsymbol{\lambda}))]^{1/2}$. Because Condition 2 in (19) involves partial derivatives, we take the partial derivative with respect to λ_n (the ' n^{th} ' tightening), so that $\frac{\partial}{\partial \lambda_n} (\boldsymbol{\lambda}_M(\mathbf{s}(\boldsymbol{\lambda})))_r = \frac{z_r^2}{(\boldsymbol{\lambda}_M)_r} \left[\mathbf{w}_r^\top \frac{\partial \mathbf{w}_r}{\partial \lambda_n} \right]$, denoting $(\boldsymbol{\lambda}_M(\mathbf{s}(\boldsymbol{\lambda})))_r = (\boldsymbol{\lambda}_M)_r$ in the right hand side. This expression provides a basis for what the matrix of partial derivatives will look like. For indices $1 \leq r, n \leq 2N$ the elements of the matrix of *sensitivities* with respect to the vector $\boldsymbol{\lambda}$ is

$$\left(\frac{\partial \boldsymbol{\lambda}_M}{\partial \boldsymbol{\lambda}} \right)_{rn} = \frac{z_r^2}{(\boldsymbol{\lambda}_M)_r} \left[\mathbf{w}_r^\top \frac{\partial \mathbf{w}_r}{\partial \lambda_n} \right]. \quad (23)$$

Note that since \mathbf{w}_r^\top is a row vector and $\frac{\partial \mathbf{w}_r}{\partial \lambda_n}$ is a column vector the entries in (23) can be written as

$$\mathbf{w}_r^\top \frac{\partial \mathbf{w}_r}{\partial \lambda_n} = \|\mathbf{w}_r\|_2 \left\| \frac{\partial \mathbf{w}_r}{\partial \lambda_n} \right\|_2 \cos(\phi_{rn}), \quad (24)$$

where ϕ_{rn} represents the angle between \mathbf{w}_r and $\frac{\partial \mathbf{w}_r}{\partial \lambda_n}$. Since $(\boldsymbol{\lambda}_M)_r = z_r \|\mathbf{w}_r\|_2$ therefore the elements of the matrix in (23) are

$$\frac{z_r^2}{(\boldsymbol{\lambda}_M)_r} \left[\mathbf{w}_r^\top \frac{\partial \mathbf{w}_r}{\partial \lambda_n} \right] = z_r \left\| \frac{\partial \mathbf{w}_r}{\partial \lambda_n} \right\|_2 \cos(\phi_{rn}).$$

From (22) it holds that $\left\| \frac{\partial \mathbf{w}_r}{\partial \lambda_n} \right\|_2 = \left\| \boldsymbol{\Sigma} \frac{\partial \boldsymbol{\Gamma}^\top}{\partial \lambda_n} \mathbf{e}_r \right\|_2$, which yields the subsequent inequalities

$$\left(\frac{\partial \boldsymbol{\lambda}_M}{\partial \boldsymbol{\lambda}} \right)_{rn} \leq |z_r| \|\boldsymbol{\Sigma}\|_2 \left\| \frac{\partial \boldsymbol{\Gamma}^\top}{\partial \lambda_n} \mathbf{e}_r \right\|_2. \quad (25)$$

Note that z_r and Σ are constants, with upper bounds $z_r \leq \max_{1 \leq r \leq 2N} |z_r| \equiv K_1$ and $\|\Sigma\|_2 \leq K_2$. Therefore, a bound for $\left\| \frac{\partial \Gamma^\top}{\partial \lambda_n} \mathbf{e}_r \right\|_2$ fully specifies (25), and thus the elements of $\frac{\partial \lambda_M}{\partial \lambda}$.

D. Part II: Sensitivities $\frac{\partial \mathbf{s}}{\partial \lambda_n}$ and $\frac{\partial^2 \mathbf{f}}{\partial \lambda_n \partial \mathbf{x}}$

In order to derive a bound on $\left\| \frac{\partial \Gamma^\top}{\partial \lambda_n} \mathbf{e}_r \right\|_2 = \left\| \mathbf{e}_r^\top \frac{\partial \Gamma}{\partial \lambda_n} \right\|_2$, recall that $\Gamma = \mathbf{J}^{-1}$. Therefore, note that we can make use of the identity

$$\frac{\partial}{\partial \lambda_n} \mathbf{J}^{-1} = -\mathbf{J}^{-1} \left(\frac{\partial}{\partial \lambda_n} \mathbf{J} \right) \mathbf{J}^{-1}.$$

Specifically, defining the vector $\mathbf{j}_r^\top \equiv \mathbf{e}_r^\top \mathbf{J}^{-1}$ then

$$\left\| \mathbf{e}_r^\top \frac{\partial \mathbf{J}^{-1}}{\partial \lambda_n} \right\|_2 = \left\| \mathbf{j}_r^\top \frac{\partial \mathbf{J}}{\partial \lambda_n} \mathbf{J}^{-1} \right\|_2 \leq \|\mathbf{J}^{-1}\|_2 \left\| \mathbf{j}_r^\top \frac{\partial \mathbf{J}}{\partial \lambda_n} \right\|_2 \quad (26)$$

With a bound on $\|\mathbf{J}^{-1}\|_2 \leq K_\Gamma$ (from (16)), it remains to derive an upper bound on $\left\| \mathbf{j}_r^\top \frac{\partial \mathbf{J}}{\partial \lambda_n} \right\|_2$. Next we describe the essential components for such a bound, based on the elements of the 2nd derivative matrices

$$\frac{\partial}{\partial \lambda_n} \mathbf{J}(\mathbf{s}(\lambda)) = \frac{\partial}{\partial \lambda_n} \left(\frac{\partial \mathbf{f}}{\partial \mathbf{x}} \right) = \begin{bmatrix} \frac{\partial^2 \mathbf{f}}{\partial \lambda_n \partial \mathbf{q}_G^g} & \frac{\partial^2 \mathbf{f}}{\partial \lambda_n \partial \mathbf{v}_L} & \frac{\partial^2 \mathbf{f}}{\partial \lambda_n \partial \boldsymbol{\theta}} \end{bmatrix}.$$

The elements of $\frac{\partial}{\partial \lambda_n} \left(\frac{\partial \mathbf{f}}{\partial \mathbf{x}} \right)$ can be computed from (15) once

$$\frac{\partial}{\partial \lambda_n} v_i \equiv \partial_n v_i, \quad \text{and} \quad \frac{\partial}{\partial \lambda_n} \theta_i \equiv \partial_n \theta_i, \quad (27)$$

for $1 \leq n \leq 2N$, $1 \leq i \leq N$ are known. This is the case, because $\frac{\partial}{\partial \lambda_n} (v_i c_{ki})$ and $\frac{\partial}{\partial \lambda_n} (v_i d_{ki})$, for $1 \leq k \leq N$, (in e.g., (15)) can be computed from these quantities. In order to develop expressions for the derivatives in (27) we use the vector variable \mathbf{s} (from (18)), which contain elements v_i and θ_i . Subsequently results from classical nonlinear programming theory, based on assumptions A.1 — A.3, ensure the existence of a parametrized solution to (18) with dependence on λ , defined by

$$\mathbf{a}(\lambda) \equiv \left[\mathbf{s}(\lambda)^\top \quad \boldsymbol{\mu}(\lambda)^\top \quad \boldsymbol{\rho}(\lambda)^\top \right]^\top.$$

Selecting a set of rows in $\mathbf{a}(\lambda)$ extracts $\mathbf{s}(\lambda)$ and thus also v_i and θ_i . The derivative of $\mathbf{a}(\lambda)$ w.r.t. λ can be computed from the KKT conditions

$$\begin{bmatrix} \frac{\partial}{\partial \mathbf{s}} L(\mathbf{a}(\lambda), \lambda) \\ \mathbf{f}(\mathbf{s}(\lambda)) \\ \boldsymbol{\rho}_i \mathbf{h}(\mathbf{s}(\lambda), \lambda)_i \end{bmatrix} \equiv \mathbf{G}(\mathbf{a}(\lambda), \lambda) = \mathbf{0}, \quad i \in \mathcal{A}(\mathbf{s}). \quad (28)$$

From (28) it holds that

$$\frac{\partial}{\partial \lambda_n} \mathbf{G}(\mathbf{a}(\lambda), \lambda) = \frac{\partial \mathbf{G}}{\partial \mathbf{a}} \frac{\partial \mathbf{a}}{\partial \lambda_n} + \frac{\partial \mathbf{G}}{\partial \lambda_n} = \mathbf{0},$$

and $\frac{\partial \mathbf{a}}{\partial \lambda_n} = -\left[\frac{\partial \mathbf{G}}{\partial \mathbf{a}} \right]^{-1} \frac{\partial \mathbf{G}}{\partial \lambda_n}$. Thus $\frac{\partial \mathbf{s}}{\partial \lambda_n}$ is obtained by extracting elements from $\frac{\partial \mathbf{a}}{\partial \lambda_n}$. The existence of the inverse and hence the derivatives of \mathbf{a} are guaranteed by [18, Theorem 3.2]. Because the derivatives are finite a bound of the form $\left\| \frac{\partial \mathbf{a}}{\partial \lambda_n} \right\|_2 \leq K_a$ exists, which implies $\left\| \frac{\partial \mathbf{s}}{\partial \lambda_n} \right\|_2 \leq K_a$, $\left\| \frac{\partial \mathbf{x}}{\partial \lambda_n} \right\|_2 \leq K_a$ and $|\partial_n v_i| \leq K_a$, $|\partial_n \theta_i| \leq K_a$. Having deduced bounds on the sensitivities $\partial_n v_i$ and $\partial_n \theta_i$ now the partial derivatives of

$\frac{\partial \mathbf{f}}{\partial \mathbf{x}}$ can be analyzed. Specifically, the partial derivatives of $\frac{\partial}{\partial \lambda_n} \left(\frac{\partial \mathbf{f}}{\partial \mathbf{x}} \right)$ are computed from (15) from which $\frac{\partial}{\partial \lambda_n} \left(\frac{\partial \mathbf{f}}{\partial \mathbf{q}_G^g} \right) = \mathbf{0}$. Since the power flow equations hold with equality at a solution, we simplify the summations in (15), using the definitions $p_i^{\text{net}} \equiv p_i^g - p_i^d$, $q_i^{\text{net}} \equiv q_i^g - q_i^d$, as e.g., $\sum_{k=1}^N v_k c_{ik} = \frac{p_i^{\text{net}}}{v_i}$ (and correspondingly for the other terms). Then for $1 \leq i \leq N$ and $j = N + i$ as well as $1 \leq l \leq N_L$ and $1 \leq t \leq N$

$$\begin{aligned} \frac{\partial}{\partial \lambda_n} \left(\frac{\partial \mathbf{f}}{\partial \mathbf{v}_L} \right)_{i,l} &= \begin{cases} \partial_n \left(\frac{p_i^{\text{net}}}{v_i} \right) + 2\partial_n (c_{ii} v_i) & \text{if } i = [L]_l \\ \partial_n (v_i c_{i[L]_l}) & \text{otherwise} \end{cases} \\ \frac{\partial}{\partial \lambda_n} \left(\frac{\partial \mathbf{f}}{\partial \mathbf{v}_L} \right)_{j,l} &= \begin{cases} \partial_n \left(\frac{q_i^{\text{net}}}{v_i} \right) + 2\partial_n (d_{ii} v_i) & \text{if } i = [L]_l \\ \partial_n (v_i d_{i[L]_l}) & \text{otherwise} \end{cases} \\ \frac{\partial}{\partial \lambda_n} \left(\frac{\partial \mathbf{f}}{\partial \boldsymbol{\theta}} \right)_{i,t} &= \begin{cases} -\partial_n q_i^{\text{net}} & \text{if } i = t \\ v_k d_{ik} \partial_n v_i + v_i \partial_n (v_k d_{ik}) & \text{otherwise} \end{cases} \\ \frac{\partial}{\partial \lambda_n} \left(\frac{\partial \mathbf{f}}{\partial \boldsymbol{\theta}} \right)_{j,t} &= \begin{cases} \partial_n q_i^{\text{net}} & \text{if } i = t \\ -(v_k c_{ik} \partial_n v_i + v_i \partial_n (v_k c_{ik})) & \text{otherwise} \end{cases} \end{aligned}$$

These derivatives can be bounded with limits on $\partial_n p_i^{\text{net}}$, $\partial_n q_i^{\text{net}}$, $\partial_n v_i$, $\partial_n \theta_i$, $\partial_n c_{ik}$, $\partial_n d_{ik}$, $\partial_n (v_k c_{ik})$, and $\partial_n (v_k d_{ik})$ (i.e., all elements that appear in the expression of the derivatives). Since all these individual elements are bounded by K_a , and since the c_{ik} , d_{ik} terms are bounded, too (they depend on v_i , θ_i), the maximum element will be bounded by a constant, as well. Denote this constant by K_x , then

$$\max_{1 \leq i, j \leq 2N} \left| \left(\frac{\partial}{\partial \lambda_n} \left(\frac{\partial \mathbf{f}}{\partial \mathbf{x}} \right) \right)_{ij} \right| \equiv K_x.$$

With this, since $\|\mathbf{j}_r\|_2 \leq K_\Gamma$ and $\frac{\partial^2 \mathbf{f}}{\partial \lambda_n \partial \mathbf{x}} = \frac{\partial}{\partial \lambda_n} \mathbf{J}(\mathbf{s}(\lambda))$, we obtain the upper bound

$$\left\| \mathbf{j}_r^\top \frac{\partial \mathbf{J}(\mathbf{s}(\lambda))}{\partial \lambda_n} \right\|_2 \leq 2K_\Gamma K_x N. \quad (29)$$

E. Part III: Bound on $\left\| \frac{\partial \lambda_M}{\partial \lambda} \right\|_2$ and Implications

The analysis from the previous section has implications for the convergence of Algorithm 1. In particular, since $\|\mathbf{J}(\mathbf{s}(\lambda))^{-1}\|_2 \leq K_\Gamma$ (cf. Section I-C2) a bound on the magnitude of $\frac{\partial \lambda_M}{\partial \lambda}$ can be found. By combining (25) and (29) one sees that

$$\begin{aligned} \left(\frac{\partial \lambda_M}{\partial \lambda} \right)_{rn} &\leq |z_r| \|\Sigma\|_2 \left\| \mathbf{e}_r^\top \left(\frac{\partial \Gamma}{\partial \lambda_n} \right) \right\|_2 \\ &\leq |z_r| \|\Sigma\|_2 K_\Gamma \left\| \mathbf{j}_r^\top \left(\frac{\partial \mathbf{J}}{\partial \lambda_n} \right) \right\|_2 \\ &\leq |z_r| \cdot \|\Sigma\|_2 \cdot K_\Gamma \cdot 2 \cdot K_\Gamma \cdot K_x \cdot N, \end{aligned}$$

where the second inequality is based on (26) and the third on (29). Since typically only $N_A \ll 4N + N_L$ inequality constraints are active at the solution, and since $|z_r| \leq K_1$ the upper bound is

$$\left\| \frac{\partial \lambda_M}{\partial \lambda} \right\|_2 \leq 2 \cdot \|\Sigma\|_2 \cdot K_1 \cdot K_\Gamma^2 \cdot K_x \cdot N_A \cdot N. \quad (30)$$

If the right hand side in (30) is less than one then Condition 2 in (19) of the fixed point iteration is guaranteed to hold. In other words

$$0 \leq 2 \cdot \|\Sigma\|_2 \cdot K_1 \cdot K_\Gamma^2 \cdot K_x \cdot N_A \cdot N < 1 \quad \text{implies} \\ \text{Algorithm 1 converges.} \quad (31)$$

F. Computing a Bound Estimate

The upper bound in (30) is composed of the parts

$$\|\Sigma\|_2, \quad K_1, \quad K_\Gamma^2 \cdot K_x \cdot N_A \cdot N.$$

The quantities $\|\Sigma\|_2$ and K_1 are related to the uncertainty in the model, whereas $K_\Gamma^2 \cdot K_x \cdot N_A \cdot N$ is problem (network specification) dependent. For instance, K_1 is reduced by reducing the probability constraints in (6). Concretely, if all $\epsilon \rightarrow 1/2$ then $K_1 \rightarrow 0$. Secondly, if $\|\Sigma\|_2$ is small enough (sufficiently small uncertainty) then from (19) the fixed point iteration is guaranteed to converge. Although the bounds may be known to be conservative, we show that if the uncertainty is small enough convergence is achieved. Such an insight may be useful if the uncertainty can be scaled (e.g., using shorter model horizons) so that its magnitude becomes smaller. Such conclusions apply to basically any type of Algorithm 1 as long as Σ is used in forming λ . Finally, the bound (30) includes the network dimension N . In numerical experiments, we observe that setting $\|\Sigma\|_2 \sim \mathcal{O}(1/N^2)$ enables the solution of large networks. Before applying Algorithm 1 for multiple iterations the bound in (30) can be qualitatively used to assess the convergence behavior of the method. In particular, at $k = 0$, use $\mathbf{s}^{(1)}$ to compute parts of the right hand side in (30). Computing K_Γ is available from or $K_\Gamma = \sqrt{\|\Gamma\|_1 \|\Gamma\|_\infty}$ (or a LU factorization of \mathbf{J}). The computation of K_x can be approximated by first estimating K_a from a lower bound on the smallest singular value of $\partial \mathbf{G} / \partial \mathbf{a}$ using [17] (as for (16)), calling such an estimate \hat{K}_a . Because λ appears linearly in the inequalities $\mathbf{h}(\mathbf{s}, \lambda) = \text{vec}(\mathbf{g}_1(\mathbf{s}), \mathbf{g}_2(\mathbf{s}) + \lambda)$ (for appropriately defined $\mathbf{g}_1(\mathbf{s}), \mathbf{g}_2(\mathbf{s})$) and in no other constraints, the expression $\partial \mathbf{G} / \partial \lambda_n = \text{vec}(\mathbf{0}, \mathbf{e}_n)$ simplifies. Subsequently, $K_a \sim 1/\hat{K}_a$ and $K_x = aK_a$, for a constant $a > 0$. Because the estimate for K_x may be reasonably small near a solution, and because K_x would incur extra computational expenses we set its value to $K_x \in (0, 1]$. If the computed bound, say $B^{(0)}$ exceeds a fixed threshold (say threshold = 10), set $\Sigma^{\text{Scaled}} = 1/B^{(0)}\Sigma$. Moreover, we include a scaling factor γ_g in computing the line flow constraint tightenings from (13), thus $\bar{\lambda}_{r_1} = \gamma_g \lambda_{r_1}$. Note that for $\gamma_g = 1$ no scaling is included. An overview of the constants is summarized in a table. Furthermore, the quantity $K_P = \|\Sigma\| K_\Gamma^2 N_A$ captures specific problem sensitivities to relevant factors such as magnitude of Γ and number of active constraints. This quantity can be computed at the beginning of applying Algorithm 1, is often inexpensive, and is expected to be small for guaranteed convergence. (If $\|\Sigma\|$ is not known it can be bounded by $K_2 = \sqrt{\|\Sigma\|_1 \|\Sigma\|_\infty}$)

TABLE I
COMPONENTS IN COMPUTING A BOUND ESTIMATE IN (30)

Constant	Meaning	Computation
K_1	Distribution bound ($z_r = F^{-1}(1 - \epsilon_r)$)	$\max_r z_r $
K_Γ	Magnitude inv. power flow Jac.	$\sqrt{\ \Gamma\ _1 \ \Gamma\ _\infty}$ or eq. (16)
K_x	Magnitude of power flow Jac. deriv. w.r.t λ	$\in (0, 1]$
N_A	Number of active inequality constraints (w/o deter. vars)	$\text{count}(\mathbf{h}(\mathbf{s}^{(1)}) = 0)$ (w/o constraints on \mathbf{y})
K_P	Problem sensitivity to inv. Jac. and active constraints	$\ \Sigma\ \cdot K_\Gamma^2 \cdot N_A$

IV. NUMERICAL EXPERIMENTS

This section describes numerical experiments on a set of standard IEEE test problems. Typically, solving large chance-constrained optimization problems is numerically very challenging. Even directly solving the reformulated problem in (17) with state-of-the-art general purpose methods becomes quickly intractable. Therefore, for larger networks we apply Algorithm 1 to approximately solve (17). Our implementation of Algorithm 1 uses Julia 1.1.0 [24] and the modeling libraries JuMP v0.18.6 [25] and StructJuMP [26]. In particular, in order to solve the AC-OPF problem from (2) and its modifications in Line 3 of Algorithm 1 we use the general purpose nonlinear optimization solver IPOPT [27]. The stopping criteria in Algorithm 1 are set as $\tau_q = 1 \times 10^{-3}$, $\tau_v = 1 \times 10^{-5}$, $\tau_\theta = 1 \times 10^{-5}$, $\tau_g = 1 \times 10^{-3}$. Unless otherwise stated, we set $\Sigma = \sigma \mathbf{I}$, $\sigma = 1/N^2$ and $\epsilon = \text{vec}(\epsilon_q, \epsilon_v, \epsilon_\theta, \epsilon_g) = \text{vec}(0.1, 0.1, 0.1, 0.2)$, and $\gamma_g = 1/N_L^2$. The initial values are computed as the midpoint between the upper and lower bounds $\mathbf{s}^{(0)} = 1/2(\mathbf{u} + 1)$. The maximum number of iterations for Algorithm 1 is set as 50. The test cases are summarized in Table II: The numerical experiments are divided into three

TABLE II
TEST CASES. COLUMN 2 CONTAINS THE TOTAL NUMBER OF NODES IN THE NETWORK, N , AND THEIR SPLIT AMONG GENERATORS, N_G , AND LOADS, N_L . THE LARGEST CASE CONTAINS MORE THAN 9000 NODES.

Problem	$N = N_G + N_L$	N_{line}	Reference
IEEE 9	9 = 3 + 6	9	[6]
IEEE 30	30 = 6 + 24	41	[6], [28]
IEEE 118	118 = 54 + 64	186	[6]
IEEE 300	300 = 69 + 231	411	[6]
IEEE 1354pegase	1354 = 260 + 1094	1991	[29]
IEEE 2383wp	2383 = 327 + 2056	2896	[6]
IEEE 2869pegase	2869 = 510 + 2359	4582	[29]
IEEE 9241pegase	9241 = 1445 + 7796	16049	[29]

parts. Experiment I compares solutions to (17) using a direct solver (i.e., IPOPT) or the iterative approach from Algorithm 1. Experiment II reports results on the test problems from Table II. Experiment III describes convergence tests according to our analysis, outcomes for problems with perturbed loads and an investigation of joint and disjoint relative frequencies on the IEEE 9 problem.

A. Experiment I

This experiment compares the optimal objective function values of solving (17) directly (CC-Direct) using IPOPT or

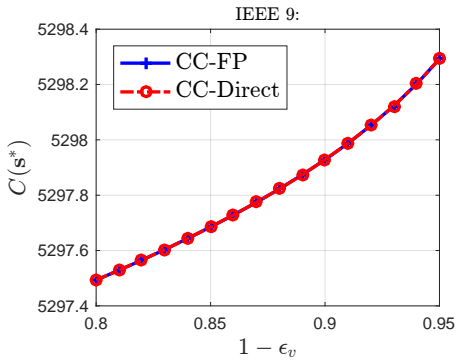


Fig. 1. Comparison of optimal objective function values using CC-Direct (direct approach) and CC-FP (fixed-point). The optimal objective function values nearly coincide on this IEEE 9 bus case as the parameters ϵ_v (probability thresholds) vary.

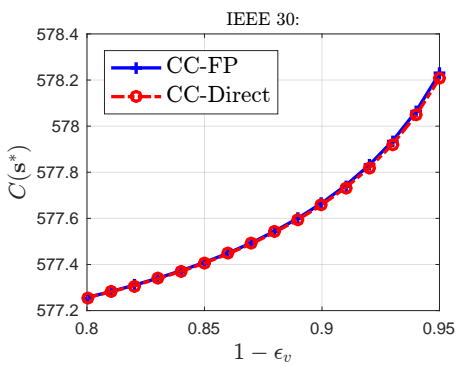


Fig. 2. Comparison of optimal objective function values using CC-Direct (direct approach) and CC-FP (fixed-point). Also on this IEEE 30 bus case the optimal objective function values nearly coincide as the parameters ϵ_v (probability thresholds) vary.

using Algorithm 1 with a fixed point approach (CC-FP). Solving (17) in JuMP becomes computationally intractable beyond $N = 100$, because the inverse, $\Gamma(\mathbf{s}) \in \mathbb{R}^{2N \times 2N}$, and its derivatives are continuously recomputed. For this reason, we compare CC-Direct and CC-FP for the 9 bus and 30 bus cases (which are both tractable by the direct approach). For the purpose of this comparison we switched the line flow tightening off (i.e., $\lambda_g = \mathbf{0}$) while all other tightenings are applied. In particular, we compare the solved objective function values after perturbing the problem formulation slightly. Specifically, we compare the computed objective function values when the values $\epsilon_v = \{0.05, 0.06, \dots, 0.2\}$ change the probability constraints. (Varying other parameters yields similar results). The outcomes of the 9 bus network are in Figure 1. Figure 2 contains the outcomes of applying both approaches on the 30 bus network. Observe in both figures that the optimal objective function values, i.e., $C(\mathbf{s}^*)$, increase as the values of $1 - \epsilon_v$ increase. This is because larger values of $1 - \epsilon_v$ correspond to stricter chance constraints. Importantly, observe that the objective function values are virtually equivalent for these test cases, as the values of the blue and red curves nearly exactly match up. However, the main advantage of Algorithm 1 is that it scales to larger cases, too.

TABLE III
COMPARISON OF ALGORITHM 1 (CC-FP) AND A DIRECT SOLUTION APPROACH (CC-DIRECT) ON A SET OF IEEE POWER NETWORKS. THE LAST 6 ROWS IN THE “OBJECTIVE” COLUMN FOR CC-DIRECT ARE LABELED N/A, BECAUSE THIS APPROACH TOOK COMPUTATIONAL TIMES IN EXCESS OF 5 HOURS.

IEEE	CC-FP			CC-Direct	
	Its.	Obj. (Cost/h)	Time(s)	Obj. (Cost/h)	Time(s)
9	4	5297.928	0.0504	5297.928	0.3075
30	4	577.6665	0.1688	577.6592	148.36
118	3	129662.0	0.4710	N/A [†]	>5h
300	5	720090.3	4.3123	N/A [†]	>5h
1354	3	74069.38	75.039	N/A [†]	>5h
2383	3	1868551.	236.27	N/A [†]	>5h
2869	3	133999.3	316.80	N/A [†]	>5h
9241	3	315912.6	3255.2	N/A [†]	>5h

B. Experiment II

Experiment II reports results of applying Algorithm 1 (CC-FP) and a direct solver (CC-Direct) to the problem from (17) on the test problems in Table II. For CC-FP the number of iterations, time and “optimal” objective values are reported. For CC-Direct the “optimal” objective values and the time are reported. Algorithm 1 converged on all of the reported problems. These problems include large network instances, too. Observe in Table III that for problems on which both solvers can be used, the optimal objective function values are close to each other. However, for large problems only Algorithm 1, based on a fixed point iteration, is practical. For consistency with Figs. 1 and 2 the line flow tightenings are switched off in the first two cases, while all tightenings are applied on all other problems.

C. Experiment III

In this experiment we investigate three further important aspects of the analysis and the algorithm. Before proceeding, we note that in Algorithm 1 it can happen that the constraint tightenings become large enough that adjusted upper bound constraints fall below a lower bound constraint (or vice-versa). Since this situation implies an inconsistent constraint, we restore consistency by re-setting this particular constraint to its original, yet with a scaled feasible interval (to reflect some tightening). Use of this correction mechanism increases the robustness of the method, meaning that Algorithm 1 converges more often. Nevertheless, our analysis indicates that a sufficiently small value of $\|\Sigma\|$ will guarantee convergence. However, other network dependent factors such as $\|\Gamma\|$ or N_A (number of active constraints) are also relevant for convergence on specific problems. We capture the conclusion that a sufficiently small $\|\Sigma\|$ guarantees convergence, and that relatively large values of $\|\Gamma\|$ and N_A typically result in non-convergence using all test problems from Table II.

1) *Experiment III.A:* This experiment varies the default value $\sigma = 1/N^2$ as $\sigma = \alpha/N^2$ with $\alpha = \{1, 10^2, 10^4, 10^6, 10^8\}$. For a sufficiently small value of σ (here $\alpha = 1$) all problems are guaranteed to converge. Moreover, lower values of $\|\Gamma\|$ and N_A represent lower sensitivity

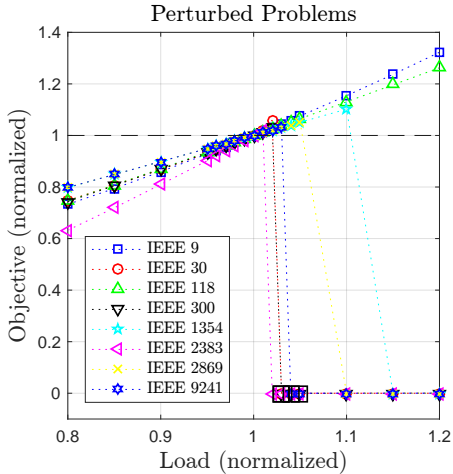


Fig. 3. Normalized optimal objective values (relative to the original optimal value), when nonzero loads at all buses in all systems vary by a factor of 0.8 — 1.2. Objective values of 0 indicate that the problem did not converge. All problems were solvable with load values up to one percent of the original. Some problems such as IEEE 9 and IEEE 118 were solvable with increases of up to 20%. Black squares represent problems in which the corresponding classical ACOPF problem (without a probability model) did converge on the same perturbed problem. In only 4 instances out of 136 total perturbed problems did this occur. Overall, the changes in loads linearly affect the optimal values and the chance-constrained models have similar sensitivities to load changes as the classical ACOPF.

of a problem to increases in $\|\Sigma\|$. Table IV reports the outcomes on all test problems. This table contains explicit values for all parameters from Table III. Thus the bound estimate from (30) can be computed. Particularly, note that when $\alpha = 1$ all the bounds are < 1 (cf. the row labeled Cond. 30). Moreover, when $\alpha = 10$ all problems with bound estimate < 1 converged (i.e., IEEE {9,118,1354,2869,9241}). This is consistent with (31). Since Condition 2 in (19) is sufficient and our analysis develops an upper bound, networks with bound estimate larger than 1 many also converge. However, when the upper bound is less than 1 then convergence of Algorithm 1 is implied. Additionally, problems IEEE {1354,2869} have the smallest K_P values indicating their tolerance to larger σ values. Problem IEEE 300 has the largest K_P value and is viewed as being more sensitive to non-convergence. Ultimately all problems are non-convergent. Prior to this IEEE {1354,2869} tend to converge on more instances while these networks have the smallest K_P values.

2) *Experiment III.B:* This experiment investigates outcomes on all test problems when loads are perturbed (representing stressed system conditions). In particular, the algorithm is applied to all problems with loads varying between 80% — 120% of their original values. Figure 3 displays the outcomes in which optimal objective values relative to the original optimal value are compared. Overall, the optimal objective values exhibit a linear relation with changes in the loads.

3) *Experiment III.C:* This experiment investigates the relation of joint and individual (disjoint) probabilities. For the IEEE 9 bus case, we sample 500 multivariate random vectors ω^p, ω^q with zero mean and positive definite dense covariance. The voltage constraints on generator buses (for this 9 bus case i.e., 1,2 and 3) are deterministic $v_j \leq u_j, j = 1, 2, 3$.

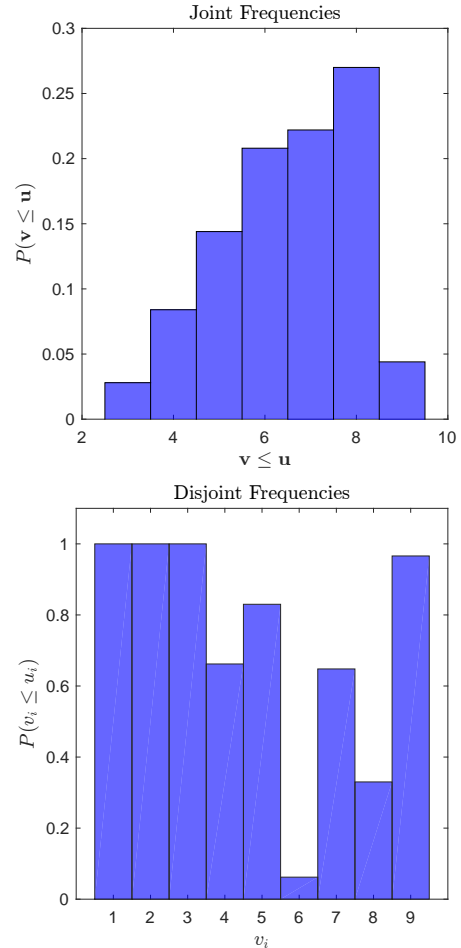


Fig. 4. Top: Relative frequencies for the count of elements of vector \mathbf{v} that satisfy $\mathbf{v} \leq \mathbf{u}$. The constraint that all 9 voltages simultaneously satisfy the inequality has probability of 0.044. Bottom: Relative frequencies of each individual voltage to satisfy its constraint. Independently enforcing each voltage to satisfy the constraints $\prod_{i=1}^9 P(v_i \leq u_i)$ has a probability of 0.007. In this case there is a factor of about 6 (i.e. 0.044/0.007) between enforcing a joint or individual constraints. However, enforcing joint probability constraints as part of an optimization for large problems is typically not computationally feasible.

The voltages at the remaining load buses are unbounded. The problem is re-solved after random loads $\mathbf{p}^d + \omega^p$ and $\mathbf{q}^d + \omega^q$ are simulated. The joint relative frequencies of the vector constraint $\mathbf{v} \leq \mathbf{u}$ (the constant vector \mathbf{u} has elements $u_i = 1.1$) are displayed on the top of Figure 4. The individual relative frequencies for each bus are at the bottom of the figure.

V. CONCLUSION

We briefly summarize limitations and future work of the analysis before concluding.

A. Limitations

Recall that Condition 2 in (19) is a sufficient condition for convergence of a fixed point iteration (such as Algorithm 1). This means that even when the condition does not hold the algorithm may still converge. In particular, when the upper bound in (30) exceeds one the algorithm may still converge.

TABLE IV
 CONVERGENCE OF ALGORITHM 1 WHEN $\sigma = \frac{\alpha}{N^2}$ FOR $\alpha = \{1, 10, 10^4, 10^6, 10^8\}$. A BOXED Y IN ROWS LABELED CONV. INDICATES CONVERGENCE. VALUES IN ROWS LABELED COND. 30 CORRESPOND TO THE COMPUTED VALUE IN THE RIGHT HAND SIDE OF (30). BOLD OR RESP. ITALIC K_P VALUES REPRESENTS THE SMALLEST RESP. SECOND SMALLEST K_P VALUES.

K_1	IEEE	K_x	K_Γ	N_A		α				
						1	10	10^4	10^6	10^8
1.3	9	0.005	1.6	2	σ	0.012	0.12	1.2e+02	1.2e+04	1.2e+06
					K_P	0.063	0.63	6.3e+02	6.3e+04	6.3e+06
					Conv.	Y	Y	Y	N	N
	Cond. 30	0.0072	0.072	72	7.2e+03	7.2e+05				
	30	0.1	8.5	1	σ	0.0011	0.011	11	1.1e+03	1.1e+05
					K_P	0.08	0.8	8e+02	8e+04	8e+06
					Conv.	Y	N	N	N	N
	Cond. 30	0.62	6.2	6.2e+03	6.2e+05	6.2e+07				
	118	0.005	6.3	16	σ	7.2e-05	0.00072	0.72	72	7.2e+03
					K_P	0.045	0.45	4.5e+02	4.5e+04	4.5e+06
Conv.					Y	Y	N	N	N	
Cond. 30	0.069	0.69	6.9e+02	6.9e+04	6.9e+06					
300	0.005	23	31	σ	1.1e-05	0.00011	0.11	11	1.1e+03	
				K_P	0.19	1.9	1.9e+03	1.9e+05	1.9e+07	
				Conv.	Y	N	N	N	N	
Cond. 30	0.73	7.3	7.3e+03	7.3e+05	7.3e+07					
1354	0.02	5.1	90	σ	5.5e-07	5.5e-06	0.0055	0.55	55	
				K_P	<i>0.0013</i>	<i>0.013</i>	<i>13</i>	<i>1.3e+03</i>	<i>1.3e+05</i>	
				Conv.	Y	Y	Y	Y	N	
Cond. 30	0.089	0.89	8.9e+02	8.9e+04	8.9e+06					
2383	0.001	45	253	σ	1.8e-07	1.8e-06	0.0018	0.18	18	
				K_P	0.092	0.92	9.2e+02	9.2e+04	9.2e+06	
				Conv.	Y	Y	Y	N	N	
Cond. 30	0.56	5.6	5.6e+03	5.6e+05	5.6e+07					
2869	0.01	5.9	185	σ	1.2e-07	1.2e-06	0.0012	0.12	12	
				K_P	0.00078	0.0078	7.8	7.8e+02	7.8e+04	
				Conv.	Y	Y	Y	Y	N	
Cond. 30	0.057	0.57	5.7e+02	5.7e+04	5.7e+06					
9241	0.002	18	511	σ	1.2e-08	1.2e-07	0.00012	0.012	1.2	
				K_P	0.002	0.02	20	2e+03	2e+05	
				Conv.	Y	Y	Y	N	N	
Cond. 30	0.093	0.93	9.3e+02	9.3e+04	9.3e+06					

However, when (30) is less than one and assumptions A.1–A.3 from Sec. III.A are satisfied then convergence is guaranteed by the fixed point theorem. Moreover, the components of (30) are computed using upper bounds or estimates as described in Table II and may thus be conservative.

B. Future Work

Since the analysis is general, it applies basically to all fixed point algorithms which iteratively re-solve power optimization problems parameterized by a sequence of constraint tightenings, $\lambda^{(k)}$. Therefore, in future work one can apply the analysis to the convergence of fixed point approaches for variations such as Robust AC Optimal Power flows, High Voltage Direct Current lines or similar problems. The decomposition of the upper bound in (30) is already detailed. Yet, new work can tighten this upper bound with sharpened estimates for the constants, and particularly the constant K_x .

In sum, this article describes a chance constrained AC optimal power flow model with only deterministic variables in the objective, which thus enables immediate interpretation of the optimal function values. By linearizing the stochastic variables, a deterministic nonlinear optimization problem is obtained in lieu of the probabilistic one. Because solving the reformulated optimization problem is computationally challenging, we develop and analyze the convergence criteria for

a fixed point algorithm that solves a sequence of modified AC optimal power flow problems and scales to larger network sizes. The analysis connects the variance of uncertainty and constraint probabilities to the convergence properties of the algorithm. In numerical experiments, we compare the fixed point iteration to directly solving the reformulated problem and test the method on IEEE problems, including a network with over 9000 nodes. Certainly our bounds are quite conservative in this version, however this is the first attempt at proving convergence of the approach. This opens up future work, since iteratively resolving a sequence of tractable optimization problems (by holding specific nonlinear terms fixed) has been very effective on a variety of power systems applications.

ACKNOWLEDGMENTS

This work was supported by the U.S. Department of Energy, Office of Science, Advanced Scientific Computing Research, under Contract DE-AC02-06CH11357 at Argonne National Laboratory and by NSF through award CNS-51545046. We acknowledge fruitful discussion with Dr. Line Roald, who pointed out that Algorithm 1 was observed to cycle between different points, and encouraged an analysis of its convergence criteria. We also thank Eric Grimm, who helped in carrying out parts of the numerical experiments in Section IV. Careful

reading and helpful suggestions of the editor and three anonymous reviewers markedly improved the manuscript.

REFERENCES

- [1] H. Zhang and P. Li, "Chance constrained programming for optimal power flow under uncertainty," *IEEE Transactions on Power Systems*, vol. 26, no. 4, pp. 2417–2424, Nov 2011.
- [2] G. Li and X. P. Zhang, "Stochastic optimal power flow approach considering correlated probabilistic load and wind farm generation," in *IET Conference on Reliability of Transmission and Distribution Networks (RTDN 2011)*, Nov 2011, pp. 1–7.
- [3] M. Hojjat and M. H. Javidi, "Chance-constrained programming approach to stochastic congestion management considering system uncertainties," *IET Generation, Transmission Distribution*, vol. 9, no. 12, pp. 1421–1429, 2015.
- [4] K. Baker, E. Dall’Anese, and T. Summers, "Distribution-agnostic stochastic optimal power flow for distribution grids," in *2016 North American Power Symposium (NAPS)*, Sep. 2016, pp. 1–6.
- [5] M. Vrakopoulou, M. Katsampani, K. Margellos, J. Lygeros, and G. Andersson, "Probabilistic security-constrained ac optimal power flow," in *2013 IEEE Grenoble Conference*, June 2013, pp. 1–6.
- [6] R. D. Zimmerman, C. E. Murillo-Sánchez, and R. J. Thomas, "Matpower: Steady-state operations, planning, and analysis tools for power systems research and education," *IEEE Transactions on Power Systems*, vol. 26, no. 1, pp. 12–19, Feb 2011.
- [7] M. Lubin, Y. Dvorkin, and L. Roald, "Chance constraints for improving the security of ac optimal power flow," *IEEE Transactions on Power Systems*, vol. 34, no. 3, pp. 1908–1917, 2019.
- [8] D. Bienstock, M. Chertkov, and S. Harnett, "Chance-constrained optimal power flow: Risk-aware network control under uncertainty," *Siam Review*, vol. 56, no. 3, pp. 461–495, 2014.
- [9] D. Lee, K. Turitsyn, D. K. Molzahn, and L. A. Roald, "Feasible path identification in optimal power flow with sequential convex restriction," *IEEE Transactions on Power Systems*, vol. 35, no. 5, pp. 3648–3659, 2020.
- [10] V. Frolov, L. Roald, and M. Chertkov, "Cloud-ac-opf: Model reduction technique for multi-scenario optimal power flow via chance-constrained optimization," in *2019 IEEE Milan PowerTech*, 2019, pp. 1–6.
- [11] L. Roald and G. Andersson, "Chance-constrained ac optimal power flow: Reformulations and efficient algorithms," *IEEE Transactions on Power Systems*, vol. 33, no. 3, pp. 2906–2918, May 2018.
- [12] J. Schmidli, L. Roald, S. Chatzivasileiadis, and G. Andersson, "Stochastic ac optimal power flow with approximate chance-constraints," in *2016 IEEE Power and Energy Society General Meeting (PESGM)*, July 2016, pp. 1–5.
- [13] Y. Xu, M. Korkali, L. Mili, J. Valinejad, T. Chen, and X. Chen, "An iterative response-surface-based approach for chance-constrained ac optimal power flow considering dependent uncertainty," *IEEE Transactions on Smart Grid*, vol. 12, no. 3, pp. 2696–2707, 2021.
- [14] R. G. J. Miller, *Simultaneous Statistical Inference*. Springer-Verlag New York, 1981.
- [15] A. Roald, D. Molzahn, and A. F. Tobler, "Power system optimization with uncertainty and ac power flow: Analysis of an iterative algorithm," in *10th IREP Symp. Bulk Power Syst. Dynamics Control.*, 2017.
- [16] D. Bienstock, *Electrical Transmission System Cascades and Vulnerability*. Philadelphia, PA: Society for Industrial and Applied Mathematics, 2015. [Online]. Available: <https://epubs.siam.org/doi/abs/10.1137/1.9781611974164>
- [17] Y. Hong and C.-T. Pan, "A lower bound for the smallest singular value," *Linear Algebra and its Applications*, vol. 172, pp. 27 – 32, 1992. [Online]. Available: <http://www.sciencedirect.com/science/article/pii/0024379592900164>
- [18] A. V. Fiacco and J. Kyparisis, "Sensitivity analysis in nonlinear programming under second order assumptions," in *Systems and Optimization*, A. Bagchi and H. T. Jongen, Eds. Berlin, Heidelberg: Springer Berlin Heidelberg, 1985, pp. 74–97.
- [19] A. V. Fiacco, "Nonlinear programming sensitivity analysis results using strong second order assumptions," in *Numerical Optimization of Dynamic Systems*, L. C. W. Dixon and e. G. P. Szegő, Eds. North-Holland, Amsterdam: Springer Berlin Heidelberg, 1980, pp. 327–348.
- [20] R. Burden and J. Faires, *Numerical Analysis*. Cengage Learning, 2010. [Online]. Available: <https://books.google.com/books?id=zXnSxY9G2JgC>
- [21] S. H. Strogatz, *Nonlinear Dynamics and Chaos: With Applications to Physics, Biology, Chemistry, and Engineering*. Addison-Wesley, 1994.
- [22] W. Karush, "Minima of functions of several variables with inequalities as side conditions," Master’s thesis, Department of Mathematics, University of Chicago, Illinois, USA, 1939.
- [23] H. W. Kuhn and A. W. Tucker, "Nonlinear programming," in *Proceedings of the Second Berkeley Symposium on Mathematical Statistics and Probability*. Berkeley, Calif.: University of California Press, 1951, pp. 481–492. [Online]. Available: <https://projecteuclid.org/euclid.bsmsp/1200500249>
- [24] J. Bezanson, A. Edelman, S. Karpinski, and V. B. Shah, "Julia: A fresh approach to numerical computing," *SIAM review*, vol. 59, no. 1, pp. 65–98, 2017. [Online]. Available: <https://doi.org/10.1137/141000671>
- [25] I. Dunning, J. Huchette, and M. Lubin, "Jump: A modeling language for mathematical optimization," *SIAM Review*, vol. 59, no. 2, pp. 295–320, 2017.
- [26] M. Anitescu and G. C. Petra, "StructJuMP a block-structured optimization framework for jump," <https://github.com/StructJuMP/StructJuMP.jl> (retrieved Mar. 27th, 2019), 2019.
- [27] A. Wächter and L. T. Biegler, "On the implementation of an interior-point filter line-search algorithm for large-scale nonlinear programming," *Math. Program.*, vol. 106, pp. 25–57, 2006.
- [28] O. Alsac and B. Stott, "Optimal load flow with steady-state security," *IEEE Transactions on Power Apparatus and Systems*, vol. PAS-93, no. 3, pp. 745–751, May 1974.
- [29] S. Fliscounakis, P. Panciatici, F. Capitanescu, and L. Wehenkel, "Contingency ranking with respect to overloads in very large power systems taking into account uncertainty, preventive, and corrective actions," *IEEE Transactions on Power Systems*, vol. 28, no. 4, pp. 4909–4917, Nov 2013.



Johannes J. Brust Was with the Mathematics and Computer Science Division at Argonne National Laboratory, IL (now Department of Mathematics, University of California, San Diego). He received a M.Sc. in financial engineering from Maastricht University and a Ph.D. in applied mathematics from the University of California, Merced. His research is on effective large scale computational methods applied to optimal power flow problems.



Mihai Anitescu Is a senior computational mathematician in the Mathematics and Computer Science Division at Argonne National Laboratory and a professor in the Department of Statistics at the University of Chicago. He obtained his engineer diploma (electrical engineering) from the Polytechnic University of Bucharest in 1992 and his Ph.D. in applied mathematical and computational sciences from the University of Iowa in 1997. He specializes in the areas of numerical optimization, computational science, numerical analysis and uncertainty quantification in which he has published more than 100 papers in scholarly journals and book chapters. He is on the editorial board of the SIAM Journal on Optimization and he is a senior editor for Optimization Methods and Software, he is a past member of the editorial boards of the Mathematical Programming A and B, SIAM Journal on Uncertainty Quantification, and SIAM Journal on Scientific Computing. He has been recognized for his work in applied mathematics by his selection as a SIAM Fellow in 2019.

The submitted manuscript has been created by UChicago Argonne, LLC, Operator of Argonne National Laboratory ("Argonne"). Argonne, a U.S. Department of Energy Office of Science Laboratory, is operated under Contract No. DE-AC02-06CH11357. The U.S. Government retains for itself, and others acting on its behalf, a paid-up nonexclusive, irrevocable worldwide license in said article to reproduce, prepare derivative works, distribute copies to the public, and perform publicly and display publicly, by or on behalf of the Government. The Department of Energy will provide public access to these results of federally sponsored research in accordance with the DOE Public Access Plan. <http://energy.gov/downloads/doe-public-accessplan>